

Metalorganic chemical vapor deposition of InGaN layers on ZnO substrates

Shen-Jie Wang, Nola Li, and Eun-Hyun Park

*School of Electrical and Computer Engineering, Georgia Institute of Technology, Atlanta, Georgia 30332-0250, USA*Siou-Cheng Lien and Zhe Chuan Feng^{a)}*Institute of Photonics and Optoelectronics and Department of Electrical Engineering, National Taiwan University, Taipei, Taiwan 106-17, Republic of China*

Adriana Valencia and Jeff Nause

*CERMET Inc., 1019 Collier Road, Atlanta, Georgia 30318, USA*Ian Ferguson^{b)}*School of Electrical and Computer Engineering, Georgia Institute of Technology, Atlanta, Georgia 30332-0250, USA*

(Received 30 July 2007; accepted 1 October 2007; published online 29 November 2007)

InGaN layers have been grown on (0001) ZnO substrates by metalorganic chemical vapor deposition utilizing a low temperature grown thin GaN buffer. Good quality InGaN films with a wide range of In composition were confirmed by high-resolution x-ray diffraction. Even at high indium concentrations no In droplets and phase separation appeared, possibly due to coherent growth of InGaN on ZnO. Photoluminescence showed broad InGaN-related emissions with peak energy lower than the calculated InGaN band gap, possibly due to Zn/O impurities diffused into InGaN from the ZnO substrate. An activation energy of 59 meV for the InGaN epilayer is determined. © 2007 American Institute of Physics. [DOI: [10.1063/1.2817482](https://doi.org/10.1063/1.2817482)]

I. INTRODUCTION

ZnO is a wurtzite semiconductor with a small *c*-plane lattice mismatch of 1.8% compared to wurtzite GaN. InGaN, with a composition of 18% In, possesses a perfect lattice match with ZnO in the *a*-axis direction according to Vegard's law and, hence, allows for the possible growth of InGaN layers without misfit dislocations.^{1,2} ZnO has a similar thermal expansion coefficient with GaN which allows for almost zero thermal strain.³ In addition, ZnO substrates are conductive so they can be utilized in vertical structures allowing for multiple electrodes to be formed on both surfaces to further current spreading.^{4,5} Furthermore, ZnO can be wet-etched chemically and easily removed to allow for a thin GaN structure.^{6,7} Therefore, ZnO is an ideal alternative substrate for GaN and InGaN based devices compared to growth on sapphire or SiC. Previously, molecular beam epitaxy and pulse laser deposition techniques have been employed to realize the low temperature epitaxy of GaN-based materials on ZnO substrates.^{1,2,8}

However, metalorganic chemical vapor deposition (MOCVD) is currently the dominant growth technology for GaN-based materials and devices and there is a need to explore this technique for ZnO substrates. It is well known that the decomposition of ZnO substrates leads to an increase in Zn and O diffusion during high temperature growth, which can result in poor epitaxial growth and degrade the film quality.^{1,2,8} This issue also has been demonstrated by second-

ary ion mass spectrometry depth profile of the GaN/ZnO interface.^{9,10} Commercial MOCVD usually grows over 1000 °C for GaN on sapphire substrates, which makes it difficult for MOCVD growth of GaN and InGaN on ZnO substrates. So far, only one group has reported the MOCVD growth of GaN on ZnO, which showed x-ray diffraction (second order) and photoluminescence (PL) peaks from GaN layer.¹¹

In this study, the growth of InGaN layers on (0001) ZnO substrates by MOCVD is reported. The grown InGaN layers contained high In composition in the range of 17%–27%, which are suitable for typical InGaN multiple quantum wells (MQWs) light emitting diode device applications. It is demonstrated that this achievement is the use of a low temperature thin GaN buffer layer to grow InGaN films on ZnO substrates.

II. EXPERIMENT

InGaN films were grown on the Zn face of (0001) ZnO substrates by MOCVD in a modified commercial rotating disk reactor with dual injector blocks. A low temperature GaN buffer layer was grown at 530 °C with a thickness of about 30 nm using trimethylgallium and ammonia as the gallium and nitrogen sources, respectively. Following the buffer, InGaN layers of about 70 nm thick were grown at temperatures ranging from 680 to 720 °C by introducing trimethylindium and triethylgallium into the reactor. N₂ carrier gas was used during the whole growth process in order to avoid etching of the ZnO surface. By varying the growth temperature, the In concentration and growth rate of the investigated films were varied from 17% to 27% and 0.16 to 0.2 μm/h, respectively. The structure and In composition of

^{a)}Also at School of Electrical and Computer Engineering, Georgia Institute of Technology (sabbatical visiting). Electronic mail: zcfeng@cc.ee.ntu.edu.tw.

^{b)}Electronic mail: ian.ferguson@ece.gatech.edu.

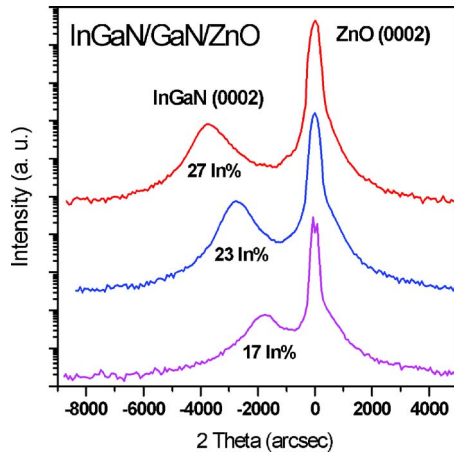


FIG. 1. (Color online) HRXRD $2\theta/\omega$ scan of InGaN layers with different In composition grown on ZnO substrates by MOCVD.

the InGaN layers were characterized by high-resolution x-ray diffraction (HRXRD) using a Philips X'Pert Pro MRD diffractometer. Optical properties were measured by room temperature and temperature-dependant PL. The field-emission scanning electron microscopy (FE-SEM) was utilized to evaluate the surface morphologies of the InGaN films.

III. RESULTS AND DISCUSSION

Figure 1 shows HRXRD (first order) $2\theta/\omega$ scans from three samples, each consisting of two well-separated peaks from the ZnO substrate and InGaN layers, respectively. The concentration of In from the InGaN layer was calculated by the shift of the (0002) InGaN peak position relative to the (0002) ZnO peak position (set at 0 arcsec) via Vegard's law. The variation of In incorporation in the InGaN layers was adjusted by changing growth temperature. The InGaN films showed single crystal diffraction peaks by $2\theta/\omega$ scans corresponding to the 17%, 23%, and 27% In content with the samples grown at 720, 700, and 680 °C, respectively. All XRD patterns revealed the small shoulder close neighbor on the right of the ZnO peaks which might be from the diffraction of the GaN buffer layer. Remarkably, only InGaN and ZnO peaks appeared in all the samples and no extra peaks were observed even in samples with composition as high as 27%. This meant no In droplets or phase separation were detected by XRD from the InGaN layers. In addition, all samples have been examined by FE-SEM with mirrorlike InGaN surfaces and no evidence of In droplets on the surface, as shown in Fig. 2.

For InGaN grown on thick GaN coated sapphire, the phase separation was widely reported for high In composition, caused by spinodal decomposition. However, for our InGaN films grown on the ZnO substrate, In droplets or phase separation were not detected by HRXRD, in contrast to the earlier cases.^{12,13} From theoretical calculation and experimental observation, biaxial strain in the epilayer is helpful in suppressing the phase separation in InGaN materials.^{14,15} Phase separation easily occurs when the InGaN layer starts to relax due to compressive strain from thick GaN/sapphire. Here, the observed suppression of phase separation in the film is believed to be due to a higher strain

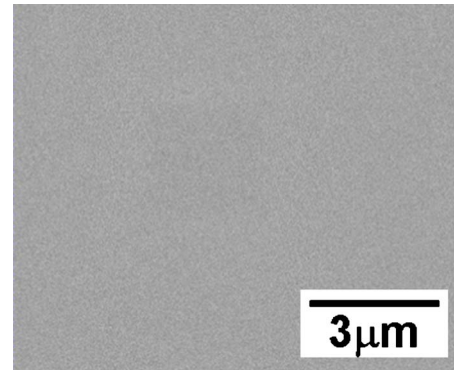


FIG. 2. (Color online) FE-SEM image of InGaN surface grown on ZnO substrates at 700 °C by MOCVD.

state of InGaN with high In content compared with the InGaN/thick GaN/sapphire materials system. The InGaN layer may stay completely strained on the thin GaN buffer, which is coherently grown on the underlying ZnO, with high In composition, since InGaN consisting of 18% In is exactly lattice matched with ZnO. As a result, a higher strain state in InGaN films with a high In concentration will be provided by ZnO compared with those grown on thick GaN/sapphire to retard the phase separation. This discrepancy is possibly caused from the different strain relaxation mechanisms in thin GaN/ZnO and thick GaN/sapphire substrate.

Figure 3 shows the room temperature PL spectra of these three samples. The emissions from the InGaN layers with different In compositions and from the ZnO substrate are observed. For the samples with an In composition of 17%, 23%, and 27%, the emission peaks were observed at 2.4, 2.1, and 1.9 eV, respectively. Assuming the 70 nm InGaN layers were strained and employing the reported band gap expression, $E_g = 3.42 - (0.65)x - 3.4159x(1-x)$,¹⁶ where x is the composition of In, the band edge emission energy can be calculated if the In concentration is known. Using the $x(\text{In})$ values of 17%, 23%, and 27% from HRXRD measurements in Fig. 1, the calculated PL peak energies of 2.8, 2.6, and 2.5 eV are obtained, respectively, which are quite different from

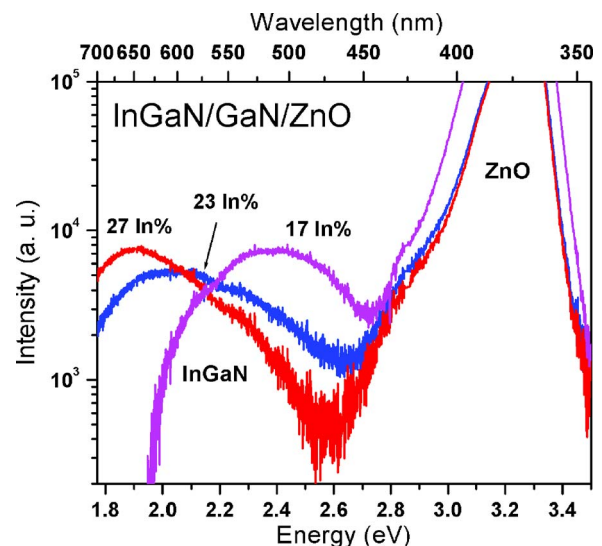


FIG. 3. (Color online) Room temperature PL spectra of InGaN films with different In composition grown on ZnO substrates by MOCVD.

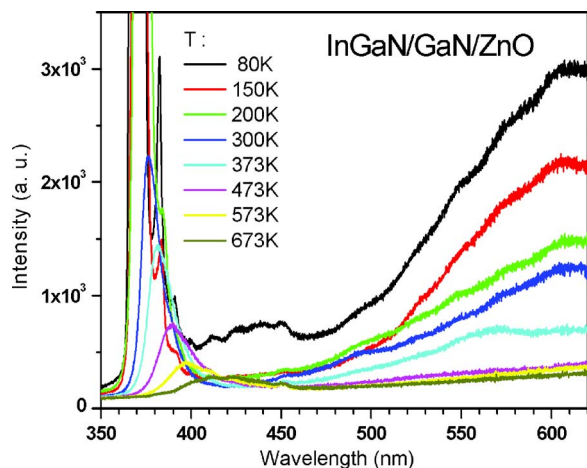


FIG. 4. (Color online) Temperature-dependent PL spectra (80–673 K) of InGaN film grown on the ZnO substrate at 700 °C.

the experimental PL results in Fig. 3. Each calculated PL peak for the InGaN layer shifts from the experimental spectral PL peak by about 0.4–0.6 eV. The lower energy PL emissions may be due to Zn and O diffusion from ZnO into the InGaN layers forming impurity levels inside the band gap emitting light with energy lower than the InGaN energy gap. It also has been observed that intentionally Zn doped InGaN shows values between 0.4 and 0.5 eV lower than calculated and experimental band gap energy of $\text{In}_x\text{Ga}_{1-x}\text{N}$ without Zn doping.¹⁷ A high density diffusion of Zn and O impurities into InGaN might also be a contributing factor to the broad full width half maximum seen in PL.

To further verify the InGaN related PL emission, temperature-dependant PL was done over a wide range of temperature from 80 to 673 K for the InGaN film grown at 700 °C, with $x(\text{In})$ of 23%, Fig. 4. The variation in intensity of InGaN (below 630 nm) with temperature is seen in this region. It shows that the PL intensity decreases with an increase in temperature, slowly at the low temperature region of 80–300 K but rapidly at the high temperature region of 373–673 K. Figure 5 exhibits the Arrhenius plot of InGaN-related PL peak intensity versus temperature in the range of 80–673 K. Best fitting leads to an activation energy, E_a , of about 59 meV for InGaN with 23% In content. Smith *et al.*¹⁸

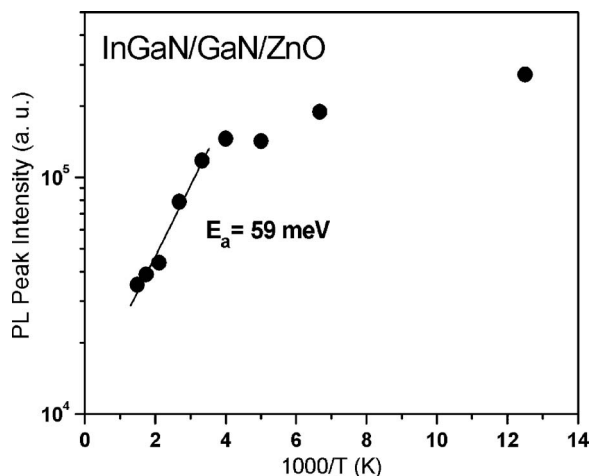


FIG. 5. PL intensity vs temperature (80–673 K) of the InGaN layer.

report an $E_a=56$ meV for the $\text{In}_x\text{Ga}_{1-x}\text{N}$ epilayer with $x=0.12$ and Teo *et al.*¹⁹ report on $\text{In}_{0.2}\text{Ga}_{0.8}\text{N}$ MQWs with an E_a value of 63 meV. The data reported in this paper are close to the earlier reported values in literature.

IV. CONCLUSIONS

In summary, MOCVD technology has been employed for the epitaxial growth of InGaN layers on (0001) ZnO substrates. This was achieved with the use of a low temperature grown thin GaN buffer layer. Good quality InGaN films with a range of high In composition of 17%–27%, as determined by high-resolution x-ray diffraction, have been obtained with growth temperatures of 680–720 °C. The InGaN films show no In droplets or phase separation. The lack of phase separation has been attributed to the higher strain state in InGaN epilayers grown on ZnO substrates. Room temperature PL data for all InGaN films show a strong emission band from ZnO and broad InGaN-related emissions with the peak energy varying with In composition. Peak energy values of the broad emissions are measured to be less than the calculated InGaN band gap by 0.5 ± 0.1 eV. These InGaN-related emissions are most likely due to recombinations involving Zn/O impurities in InGaN due to the Zn/O diffusion from the ZnO substrate. Temperature-dependent PL measurements, 80–673 K, obtained an activation energy of 59 meV for the InGaN epilayer.

¹A. Kobayashi, J. Ohta, and H. Fujioka, J. Appl. Phys. **99**, 123513 (2006).

²G. Namkoong, S. Burnham, K. Lee, E. Trybus, W. A. Doolittle, M. Lorusso, P. Capezzuto, G. Bruno, B. Nemeth, and J. Nause, Appl. Phys. Lett. **87**, 184104 (2005).

³F. Hamdani, M. Yeadon, D. Smith, H. Tang, W. Kim, A. Salvador, A. E. Botchkarev, J. M. Gibson, A. Y. Polyakov, M. Skowronski, and H. Morkoc, J. Appl. Phys. **83**, 983 (1998).

⁴G. H. B. Thompson, *Physics of Semiconductor Laser Devices* (Wiley, Chichester, 1980), p. 307.

⁵A. Zukauskas, M. S. Shur, and R. Gaska, *Introduction to Solid-State Lighting* (Wiley, New York, 2002), p. 75.

⁶W. S. Wong, T. Sands, N. W. Cheung, M. Kneissl, D. P. Bour, P. Mei, L. T. Romano, and N. M. Johnson, Appl. Phys. Lett. **77**, 2822 (2000).

⁷S. C. Hsu and C. Y. Liu, Electrochem. Solid-State Lett. **9**, G171 (2006).

⁸X. Gu, M. A. Reschikov, A. Teke, D. Johnstone, H. Morkoc, B. Nemeth, and J. Nause, Appl. Phys. Lett. **84**, 2268 (2004).

⁹G. Popovici, W. Kim, A. Botchkarev, H. Tang, H. Morkoc, and J. Solomon, Appl. Phys. Lett. **71**, 23 (1997).

¹⁰T. Suzuki, C. Harada, H. Goto, T. Minegishi, A. Setiawan, H. J. Ko, M. W. Cho, and T. Yao, Curr. Appl. Phys. **4**, 643 (2004).

¹¹R. Paszkiewicz, B. Paszkiewicz, R. Korbutowicz, J. Kozłowski, M. Tlaczala, L. Bryja, R. Kudrawiec, and J. Misiewicz, Cryst. Res. Technol. **36**, 971 (2001).

¹²N. A. El-Masry, E. L. Piner, S. X. Liu, and S. M. Bedair, Appl. Phys. Lett. **72**, 40 (1998).

¹³Z. C. Feng, T. R. Yang, R. Liu, and T. S. A. Wee, Mater. Sci. Semicond. Process. **5**, 39 (2002).

¹⁴A. Tabata, L. K. Teles, L. M. R. Scolfaro, J. R. Leite, A. Kharchenko, T. Frey, D. J. As, D. Schikora, K. Lischka, J. Furthmüller, and F. Bechstedt, Appl. Phys. Lett. **80**, 769 (2002).

¹⁵S. Y. Karpov, MRS Internet J. Nitride Semicond. Res. **3**, 16 (1998).

¹⁶C. A. Parker, J. C. Roberts, S. M. Bedair, M. J. Reed, S. X. Liu, N. A. El-Masry, and L. H. Robins, Appl. Phys. Lett. **75**, 2566 (1999).

¹⁷S. Nakamura, J. Cryst. Growth **145**, 911 (1994).

¹⁸M. Smith, G. D. Chen, J. Y. Lin, H. X. Jiang, M. Asif Khan, and Q. Chen, Appl. Phys. Lett. **69**, 2837 (1996).

¹⁹K. L. Teo, J. S. Colton, P. Y. Yu, E. R. Weber, M. F. Li, W. Liu, K. Uchida, H. Tokunaga, N. Akutsu, and K. Matsumoto, Appl. Phys. Lett. **73**, 1697 (1998).